J. Braz. Chem. Soc., Vol. 10, No. 2, 97-103, 1999.
Printed in Brazil.

0103 – 5053 $6.00 + 0.00

Article

Photoacoustic Monitoring of Internal Plastification in Poly(3-hydroxybutyrate-co-3-hydroxyvalerate) Copolymers: Measurements of Thermal Parameters

***Ruben R. Sanchez*[a], *Jacques B. Rieumont*[a], *Sergio L. Cardoso*[b], *Marcelo G. da Silva*[c], *Marcelo S. Sthel*[c], *Marcelo S. O. Massunaga*[c], *Carlos N. Gatts*[c], *and Helion Vargas*[c]**

[a]*Laboratório de Materiais Avançados – LAMAV*

[b]*Laboratório de Ciências Químicas - LCQUI*

[c]*Laboratório de Ciências Físicas – LCFIS*

Universidade Estadual do Norte Fluminense, Centro de Ciência e Tecnologia,

Av. Alberto Lamego, 2000, 28015-620 Campos dos Goytacazes – RJ, Brazil

Propriedades termofísicas de copolímeros poli(3-hidroxibutirato-co-3-hidroxivalerato) poli(3HB-co-3HV) foram investigadas com o objetivo de entender a influência das unidades monoméricas de 3-hidroxivalerato (3HV) incorporadas durante a copolimerização aleatória. Os resultados mostram forte evidência de que uma plastificação interna é introduzida no copolímero pelas unidades de 3HV. Foi observado que a condutividade térmica do copolímero aumentou linearmente com a concentração de 3HV. Por outro lado, a difusividade térmica foi muito sensível as mudanças de composição do copolímero, apresentou um aumento brusco inicial e atingiu um platô de saturação. Os gráficos de amplitude contra frequência indicam a predominância de um mecanismo termoelástico. Neste trabalho é apresentando uma nova montagem fotoacústica para as medidas de efusividade térmica.

Basic data on thermophysical properties of poly(3-hydroxybutyrate-co-3-hydroxyvalerate) copolymers poly(3HB-co-3HV) were investigated with the aim of understanding the role of 3-hydroxyvalerate monomeric units (3HV) incorporated during random copolymerization. The results show strong evidence that internal plastification is produced by the introduction of 3HV units in the copolymer. It was observed that copolymer thermal conductivity increased approximately linearly with the 3HV content. On the other hand, thermal diffusivity was very sensitive to the change in the copolymer composition showing a sudden rise that attained a saturation plateau. Amplitude-frequency plots indicate that a thermoelastic bending mechanism is operating. In this paper a new photoacoustic arrangement for the measurement of thermal effusivity is presented.

Keywords: *photoacoustic spectroscopy, thermopysical parameters, poly(hydroxyalkanoates), poly(3-hydroxybutyrate-co-3-hydroxyvalerate)*

Introduction

Photoacoustic (PA) spectroscopy and related photothermal techniques[1-3] are well-established spectroscopic techniques. The PA technique, apart from providing direct optical absorption spectra[4,5], can also be used to perform depth profile analysis[4,6], and characterization of thermal properties[7,8]. In addition, there has been a substantial development of new, versatile and competitive instrumentation and experimental methodologies suitable for use in daily practice. For a comprehensive review of the photothermal wave phenomenon and its applications the reader is referred to the books by Rosencwaig[1] and Almond[3] and to some of many published reviews on the subject[2,9,10].

This paper is concerned with the use of PA methodologies to study the thermophysical properties of poly(hy-

droxyalkanoates) which are biodegradable and bio-compatible polyesters produced from various carbon substrates by microorganisms such as prokaryotic organisms, including gram-positive and gram-negative bacteria[11].

In particular, research on microbial polyesters is expanding in both the biological and polymer sciences. Furthermore these materials have attracted industrial attention as large-scale biotechnological products[12].

One of these interesting polyesters is the poly(3-hydroxybutyrate) poly(3HB), which can be obtained as homopolymer or, its copolymer with 3-hydroxyvalerate, poly(3-hydroxybutyrate-co-3-hydroxyvalerate) poly(3HB-co-3HV)[10]. Despite the large body of literature that already exists on poly(3HB-co-3HV), so far there have been no reports on the thermophysical properties of these important materials. To our knowledge diffusivity and thermal conductivity measurements are lacking in the literature for these materials. Thermal properties should contribute to the using of these materials as membranes and envelopes for complex biomaterials in medicine and also for agrotechnical and daily life purposes.

Our objective is to determine the potential of the photoacoustic technique for measuring the thermophysical properties of poly(3HB) and poly(3HB-co-3HV) polymers. The thermophysical properties of polyesters are important when predicting heat transfer rates during processing and for process control.

Materials and Methods

Sample preparation

Poly(3HB) and poly(3HB-co-3HV) copolymers (8, 14, and 22% 3HV) were obtained from Aldrich. These copolymers are produced in a fed batch fermentation process by Alcaligenes eutrophus when grown on glucose and propionic acid as the sole carbon source. This bacterium accumulates poly(3HB-co-3HV) up to 80% of the entire dry weight of the biomass by limiting a nutrient such as nitrogen while maintaining an excess of carbon source. Polymer solutions were prepared by boiling weighed sample in chloroform until dissolution. Films were prepared by spin coating from chloroform polymer solutions (1 g/10 mL) at 160 rpm. Films were separated in water and dried at room temperature overnight. The films had a thickness of roughly 20 μm.

Thermal diffusivity PA measurement

The room temperature characterization of the samples thermal properties was based upon the measurements of the thermal diffusivity, α, and the thermal effusivity, e. The thermal diffusivity, defined as alpha $\alpha = k/\rho c$, measures essentially the thermalization time within the sample, whereas, the thermal effusivity, given by $e = (k\rho c)^{1/2}$ measures the sample thermal impedance for the heat transfer. Here, k denotes the sample thermal conductivity, ρ the material density, and c the specific heat at constant pressure. The measurements of α and e determine the thermal properties of the samples. The significance of α as a physical parameter to be monitored is due to the fact that like the optical absorption coefficient, it is unique for each material. Furthermore, the thermal diffusivity is extremely dependent upon the effects of composition and micro-structural variables, as well as processing conditions as in the case of foodstuffs[7], polymers[13], semiconductors[8,14], and solvent evaporation[15]. This can be appreciated from the tabulated values of α presented by Touloukian *et al.*[16] for a wide range of materials. The thermal diffusivity can be accurately measured by the PA technique. This technique looks directly at the heat generated in a sample, due to non-radioactive de-excitation processes, following the absorption of light. In the conventional PA experimental arrangement a sample enclosed in an air-tight cell is exposed to a chopped light beam. As a result of the periodic sample heating, the pressure in the air chamber oscillates at the chopping frequency and can be detected by a sensitive microphone coupled to the cell. The PA signal depends not only on the amount of the heat generated in the sample (*i.e.*, on the optical absorption coefficient and the sample light-into-heat conversion efficiency), but also on how the heat diffuses through the sample.

The PA measurements of the thermal diffusivity have been carried out employing a different version of the PA technique. Among several techniques the OPC method was chosen. It consists of mounting the samples directly onto a cylindrical electret microphone and using the front air chamber of the microphone itself as the usual gas chamber of conventional photoacoustics, as shown in Fig. 1. As it is well known, the modulation frequency dependence of the PA signal is the usual way for extracting information about the thermal diffusivity of the material under investigation. For the present case of thermally thick samples [sample thickness l exceeds the thermal diffusion length μ =

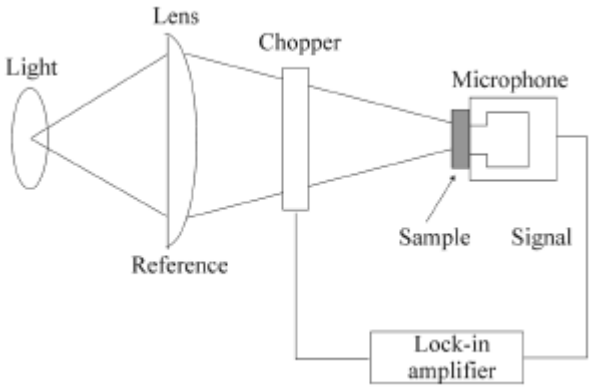

Figure 1. Schematic arrangement for the PA measurements of thermal diffusivity.

$(\alpha/\pi f)^{1/2}$, where f is the modulation frequency of the incident light] it can be shown[7,8,13] that the thermal diffusitivy α is obtainable by fitting [coefficient $a = (\pi l^2/\alpha)^{1/2}$] the measured amplitudes of the PA signal,

$$S = \frac{A}{f} e^{-a\sqrt{f}} \quad (1)$$

The constant A in Eq. (1) includes, apart from geometrical parameters, factors such as gas thermal properties, light beam intensity, and room temperature. However, for a plate shaped sample, the contribution to the PA signal from the thermoelastic bending of the sample cannot be neglected, especially for thermally thick samples as has been demonstrated by many authors. This effect is essentially due to the temperature gradient inside the sample along the z-axis[17,18]. Owing to the existence of this temperature gradient parallel to the z-axis, thermal expansion depends on z. This z-dependence of the displacement along the radial direction induces a bending of the plate in the z-direction (drum effect), *i.e.*, the vibrating sample, acts as a mechanical piston, thereby contributing to the PA signal. In the thermally thick regime, the pressure fluctuation in the air chamber of the PA cell resulting from the thermoelastic displacement of the sample is given by

$$\delta_p = \frac{3\,\alpha_T\, r_0^4\, \gamma\, P_0\, I_0\, \alpha_S}{4\,\pi\, R_c^2\, l_S^2\, l_G\, k_S\, f}\left[\left(1-\frac{1}{x}\right)+\frac{1}{x^2}\right]^{1/2} e^{j\left(\omega t+\frac{\pi}{2}+\phi\right)} \quad (2)$$

where $x = l_s a_s = l_s(\pi f/\alpha_S)^{1/2}$, $\tan\phi = 1/(x-1)$, α_T is the sample thermal expansion coefficient, R_0 is the radius of the front hole of the microphone, and R_C is the radius of the front air chamber. Eq. (2) means that the thermoelastic contribution, at high modulation frequency such that $x >> 1$, varies as f^{-1} and its phase ϕ approaches 90° as

$$\phi = \phi_0 + \arctan\left(\frac{1}{x-1}\right) \quad (3)$$

Thus for a thermally thick sample, if the thermoelastic contribution is dominant, the thermal diffusivity can be evaluated from the modulation-frequency dependence of either the signal amplitude, Eq. (2), or its phase, Eq. (3).

The PA setup for measurements of the thermal diffusivity shown in Fig. 1 consists of a 10 mW He-Ne laser, the monochromatic beam of which was modulated using a variable speed chopper (PAR, model 650) and then focused onto the sample. The output voltage of the microphone was measured using a lock-in amplifier (PAR, model 5210). To derive Eqs. (2), (3) and (4), we have assumed that the sample is optically opaque and that the heat flux into the surrounding air is negligible. The implicit optical opaqueness condition was ensured by the use of a thin circular absorbing Al foil (14 μm thick and 5 mm diameter) attached to the front of the sample using a thin layer of vacuum grease. The thermal diffusion time in this Al foil is in the order of 13.6 μs so that the heat generated in the thin Al absorber can be assumed instantaneously transmitted to the sample.

Thermal effusivity measurements

To complete the characterization of the sample thermal properties, we have measured the thermal effusivity e. Knowing e and α, the sample thermal conductivity and heat capacity per unit volume are readily obtained from the equations

$$k = e\sqrt{\alpha}$$

$$\rho\, c = \frac{e}{\sqrt{\alpha}} \quad (4)$$

The thermal effusivity was measured using a new experimental configuration schematically shown in Fig. 2. A chopped, 10 mW He-Ne laser beam after being expanded, was directed to a 14 mm diameter Al disk absorber (20 μm thick) attached to the sample with the help of a very thin adhesive layer. The role of this Al absorber is to ensure that the incident light beam generates a surface sample heating, thereby fulfilling the sample optical opaqueness condition as in the case of α measurements. The sample-absorber system closes one of the 8 mm diameter openings of a 2 mm long cylindrical cell cavity. A BK-7 glass window closes the other cavity opening. The laser beam was expanded to ensure uniform light absorption at the Al foil. An electret microphone coupled to the PA cell cavity through a 1 mm diameter column located in the cavity wall, is used to sense pressure fluctuations in the PA cavity produced by the periodic sample heating due to the pumping beam. The microphone signal is fed into a lock-in amplifier, whose output signal is recorded as a function of the modulation frequency.

The pressure fluctuations in the PA cell can be calculated using the Rosencwaig and Gersho model[1] for the

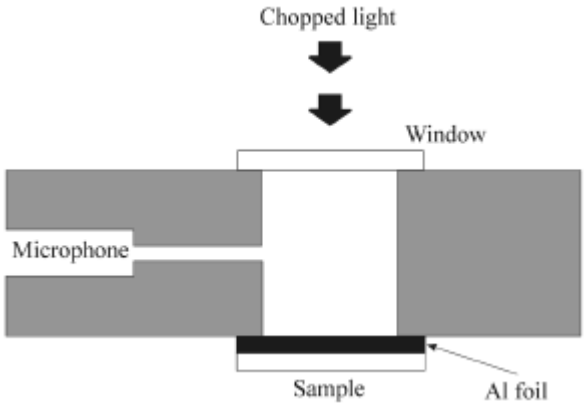

Figure 2. PA experimental setup used to measure the thermal effusivity.

photoacoustic effect similarly to the previous case of the thermal diffusivity treated above. Considering the relevant case a thermally thin Al absorber ($l_0\sigma_0 < 1$) and a thermally thick sample ($l_0\sigma_0 > 1$), for the sample-Al absorber system,

$$\delta_p = \frac{P_0 I_0}{T_0 l_G \sigma_G k_0 l_0 \sigma_0^2} \frac{1}{[1 + \frac{b}{l_0\sigma_0}]} \quad (5)$$

where the subscript 0 refers to the Al absorber and $b = e/e_0$ is the ratio of the sample to the Al foil thermal effusivity. Knowing b, the sample thermal effusivity e is readily obtained, since the aluminium thermal effusivity is well known, $e_0 = 2.47$ $Ws^{1/2}/cm^2$ K. In the absence of a sample attached to the Al foil we have $b = 0$ and Eq. (5) reduces to

$$\delta_p = \frac{P_0 I_0}{T_0 l_G \sigma_G k_0 l_0 \sigma_0^2} \quad (6)$$

which is the pressure fluctuation caused by the Al absorber. It follows from Eqs. (5) and (6) that the thermal effusivity may be directly obtained from the data fitting of the signal ratio $|\delta p/\delta p_0|$ as a function of the modulation frequency. In fact, using Eqs. (5) and (6), the signal amplitude may be written as:

$$\left|\frac{\delta p}{\delta p_0}\right| = \frac{C}{[1 + \frac{b}{z_0} + 2(\frac{b}{2z_0})^2]^{1/2}} \quad (7)$$

where the constant fitting parameter C has been introduced to account for eventual small differences in the Al foil reflectivity, and $z_0 = l_0(\pi f/\alpha_0)^{1/2}$. In Eq. (7) C and b are left as fitting parameters.

Results and Discussion

Fig. 3 shows the PA amplitude as a function of the frequency modulation for the homopolymer poly(3HB). It can be seen that for a high modulation frequency, above, say 100 Hz, the signal amplitude scales essentially as $f^{-0.9}$, a value close to f^{-1}. This f^{-1} frequency dependence of the PA signal of a thermally thick sample suggests that in this frequency range, the thermoelastic bending is the dominant mechanism responsible for the acoustic signal. Eq. (2) can therefore be used to analyze the thermal diffusivity of our poly(3HB). Accordingly, the thermal diffusivity can be evaluated using either the PA signal amplitude or phase data fitting to Eqs. (2) and (3) respectively. In this instance, Eq. (3) was used for the PA signal phase data fitting for evaluation of the thermal diffusivity. Fig. 4 shows the PA signal phase data, as a function of the modulation frequency for poly(3HB). The solid curve in this figure corresponds to the experimental phase data fitting to Eq. (3). The value of the thermal diffusivity obtained from the data fitting was 2.6×10^{-4} cm^2 s^{-1} [typical value for thermal diffusivity of a polymer specimen, $\alpha \approx 10^{-4}$ cm^2 s^{-1}]. Note that, in the frequency range (100 – 200 Hz) of our experiment, the sample was thermally thick, *i.e.*, its thermal diffusion length $(\alpha/\pi f)^{1/2}$ was much smaller than its thickness. The same procedure was applied to the other samples. The PA signal amplitude as a function of the modulation frequency was compared (Fig. 5) for the (A) 20 μm thick poly(3HB-co-3HV) sample with 8% of 3HV, (B) 20 μm thick poly(3HB-co-3HV) sample with 14% of 3HV and (C) 20 μm thick poly(3HB-co-3HV) sample with 22% of 3HV. As can be seen the PA signal scales as f^{-1}, $f^{-0.9}$, and $f^{-1.1}$ for samples (A), (B) and (C) respectively, instead of exhibiting the exponential behavior (Eq. (1)) predicted by the thermal diffusion model[1,2]. The observed frequency dependence indicates that in this frequency range, the thermoelastic bending is the dominant mechanism responsible for the acoustic signal in the thermally thick region. As before, Eq. (3) was used for the PA signal phase data fitting for evaluating the thermal diffusivity. In Fig. 6 the signal phase is

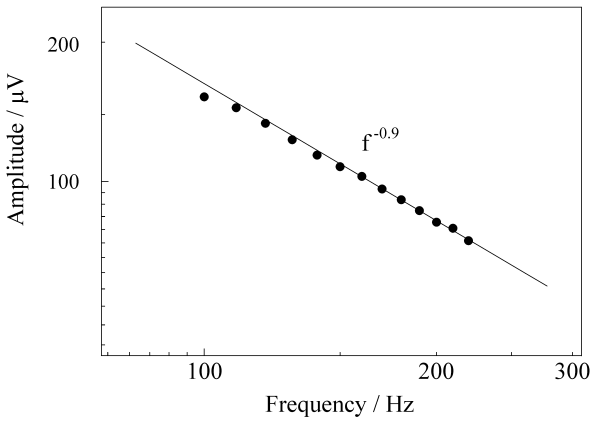

Figure 3. Modulation frequency dependence of the PA signal for the homopolymer poly(3HB).

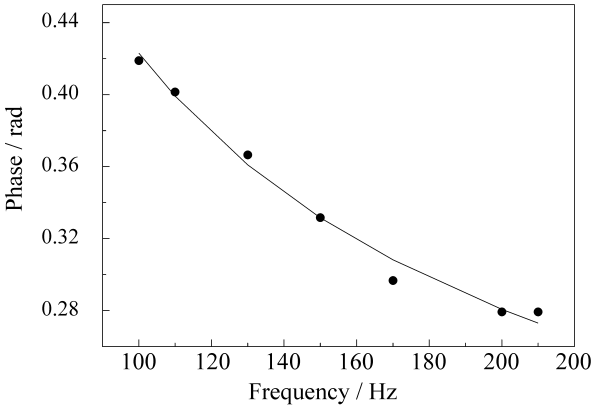

Figure 4. Dependence of PA signal phase on the chopping frequency for the homopolymer poly(3HB). The solid curve represents the experimental data fitting to Eq. (3) of the text.

shown as a function of the modulation frequency for (A) 20 μm thick poly(3HB-co-3HV) sample with 8%, (B) 14% and (C) 22% of 3HV, respectively. The solid curves in Fig. 6 represent the fit to the experimental phase data by the theoretical expression in Eq. (3). The values of the thermal diffusivity obtained from the data fitting were $\alpha = 4.6 \times 10^{-4}$ cm^2 s^{-1} for the sample with 8% of 3HV, $\alpha = 4.8 \times 10^{-4}$ cm^2 s^{-1} for the sample with 14% of 3HV and $\alpha = 4.6 \times 10^{-4}$ cm^2 s^{-1} for the sample with 22% of 3HV, respectively.

To complete the determination of the thermal properties of the sample, we have measured the thermal effusivity *e*. In Fig. 7 the signal amplitude is shown as a function of the modulation frequency in the absence of a sample attached to Al foil. We call this the reference signal. As predicted, the amplitude of the signal due to the Al foil, which is thermally thin ($l_0\sigma_0 < 1$) varies as $f^{-3/2}$. According to Eq. (7) the thermal effusivity can be obtained from the data fitting of the signal ratio $|\delta p/\delta p_0|$ as a function of the modulation frequency. Fig. 8 shows the measured ratio for poly(3HB-co-3HV) sample with 14% of 3HV as a function of the modulation frequency. The solid line in Fig. 8 represents the best fit for the data corresponding to the analytical expression (Eq. (7)). One finds a value of $e = 0.14$ $Ws^{1/2}/cm^2$ K. The same procedure for measuring the thermal effusivity was repeated with all the other polymeric samples. The data obtained from the thermal property measurements are summarized in Table 1.

The magnitude of thermal parameters (Table 1) were in the range with the values quoted in the literature for polymers[16,17-19]. There was also a consistent trend, suggesting that the values of the thermal parameters increase as the 3HV content increases and these values were larger than thermal parameters for a sample without 3HV. These changes are due to the fact that 3HB monomeric units are being replaced by the 3HV ones (see Scheme 1).

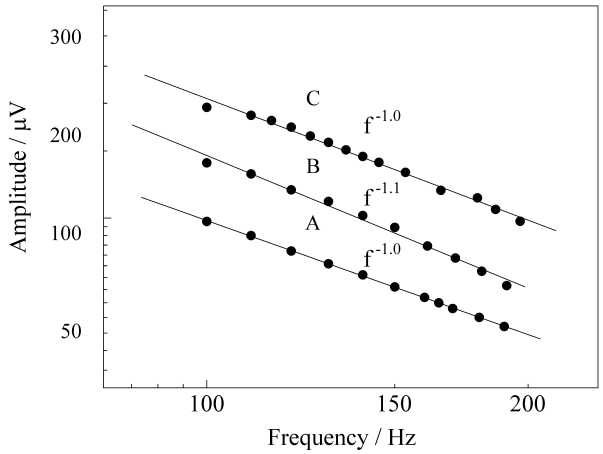

Figure 5. Modulation frequency dependence of the PA signal for poly(3HB-co-3HV) with (A) 8 % of 3HV, (B) 14 % of 3HV and (C) 22 % of 3HV.

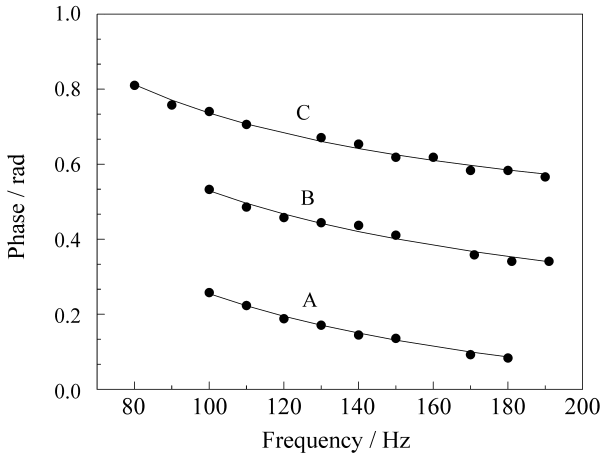

Figure 6. Dependence of PA signal phase on the chopping frequency for poly(3HB-co-3HV) with (A) 8 % of 3HV, (B) 14 % of 3HV and (C) 22 % of 3HV. The solid curve represents the experimental data fitting to Eq.(3) of the text.

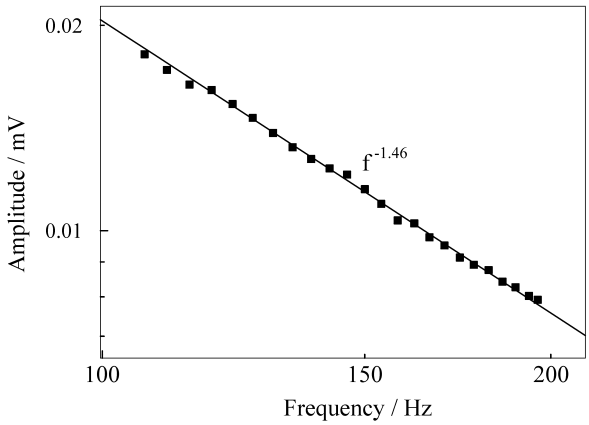

Figure 7. Signal amplitude as a function of the modulation frequency for the Al foil.

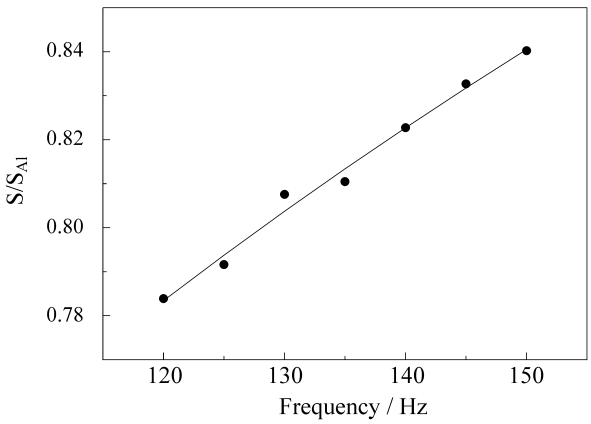

Figure 8. The amplitude ratio signal for poly(3HB-co-3HV) with 14% of 3HV as a function of the modulation frequency. The full line represents the best fit to the Eq.(7) of the text.

Table 1. Thermal parameters of poly(3HB-co-3HV) as a function of 3HV concentration. The values of the thermal concuctivity k and heat capacity per unit volume ρc were calculated from the measured values of α and *e*, using Eq. (4) of the text.

3HV Concentration (%)	α	ρc	*k*	*e*
0	2.6	11.78	3.0	0.19
8	4.6	7.93	3.5	0.17
14	4.8	6.39	3.2	0.14
22	4.6	8.39	3.9	0.18

Addition of 3HV units can be considered as an internal plastification due to the enlargement of the side group from methyl to ethyl, although this terminology is used mainly for amorphous polymers. If 3HV units are concentrated in the minor amorphous region, a decreasing trend for thermal properties would be observed. 3HV units are randomly distributed and the crystalline region is perturbed by changing a methyl group for an ethyl. These changes seem to represent a more ordered way to accommodate the ethyl group and result in increasing in thermal properties.

Figures. 9 and 10 show the experimental values of the thermal diffusivity and thermal conductivity of poly(3HB-co-3HV) as a function of 3HV content. X-ray diffraction patterns of poly(3HB-co-3HV)s show the presence of only one crystalline phase at all compositions between 0 and 47% of 3HV. This means that the segments of the chain conformation of both homopolymers can be accommodated in the orthorhombic unit cell. From the unit cell data, the volumes of the two monomer units are very similar: 0.11 nm^3 for poly(3HB) and 0.13 nm^3 for poly(3HV). This phenomenon is known as isodimorphism[10,20]. Measurements of *d* spacing from X-ray diffraction patterns indicate a slight expansion of the (110) plane as the 3HV content of the copolymer increases while the *d* spacing of the planes (020) and (002) are invariant. However, small changes in the *d* spacing for the (110) plane of poly(3HV) are not considered a significant change in the lattice because macroscopic crystalline densities estimated from lattice indices measured by wide angle X-ray scattering remained almost constant up to 50% 3HV content[21]. On the other hand, amorphous polymers are characterized by smaller thermal diffusivity than crystalline polymers[21]. As it is well known poly(3HB-co-3HV)s have glass transitions below room temperature and their values linearly decrease as the 3HV content increases producing an internal plastification of its amorphous phase[10]. It is also known that external plastification with di-alkyl phthalates of polymers such as poly(vinyl chloride) reduces the thermal conductivity[22] due to the increase of segmental chain mobility. However, amorphous polymers do not follow necessarily a trend with respect to their glass transitions. Thus, polystyrene with a higher Tg (100 °C) has a lower thermal conductivity than poly(vinyl acetate) (Tg 28 °C)[22,23]. Furthermore, the density of poly(3HB-co-3HV)s quenched in liquid nitrogen decreases with 3HV content[21]. These quenched polymers can be considered completely amorphous. In conclusion the main contribution to the thermal properties are due to

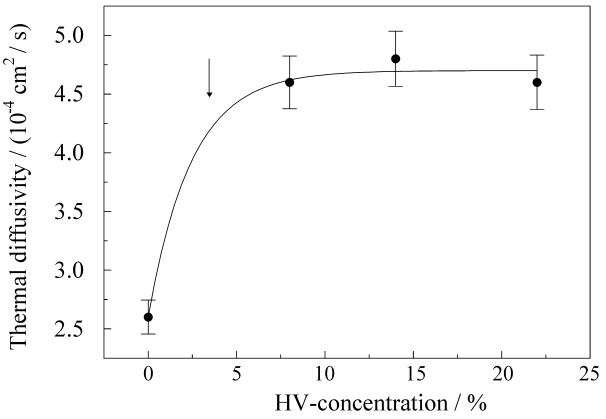

Figure 9. Thermal diffusivity of poly(3HB-co-3HV) as a function of 3HV concentration. The values are from Table 1.

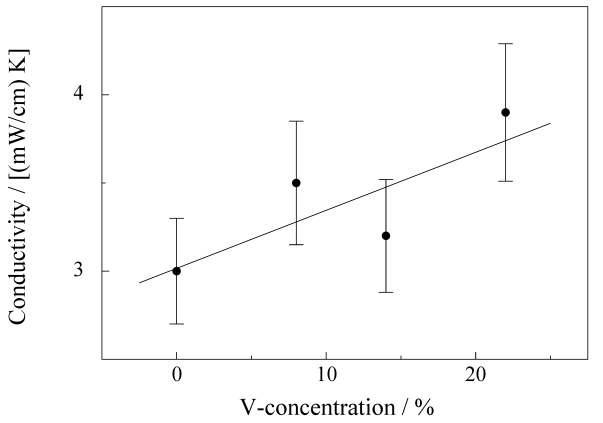

Figure 10. Thermal conductivity of poly(3HB-co-3HV) as a function of 3HV concentration. The values are from Table 1.

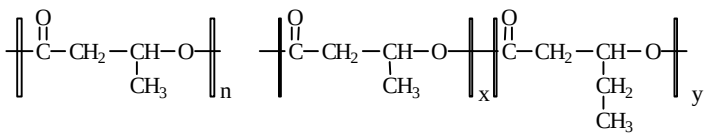

Poly(3HB) Poly(3HB-co-3HV)

Scheme 1.

the changes that occurred in the crystalline phase and not or to a minor extent in the amorphous one.

All the gathered facts indicate that some factors may be operating to increase the thermal diffusivity and conductivity as internal plastification proceeds. As the methyl group is replaced by ethyl group, local sites of greater microdensity are created. Thus the contribution of the ethyl groups, randomly distributed in the chains, is as a layer compactor allowing a concerted action of such sites making easier the energy transfer.

We also note that the data shown in Fig. 9 can be used to estimate the 3HV-concentration scale for reaching saturation of the thermal difusivity changes. This can be done by fitting the data to an exponentially growing function of the form $\alpha = \alpha_0 + \alpha_1 [1 - \exp(-HV/\tau)]$. In this expression α_0 is the thermal diffusivity of the poly(3HB) sample, α_1 is the shift in the thermal diffusivity induced by the 3HV-presence, and τ is the concentration constant for reaching saturation. Using the data of Fig. 9 we have found:

$$\alpha = 2.60 \times 10^{-4} + 2.10 \times 10^{-4} [1 - e^{-HV/2.45}] \quad (8)$$

The sum of the square of the residues and the error in this fitting were 2.17×10^{-10} and 1.18% respectively. This means that the trial function we have used indeed produces a good description of the evolution of α as a function of the 3HV-concentration. It follows from Eq. (8) that 90% of the α saturation value (*i.e.*, $\alpha = 4.23 \times 10^{-4}$ cm^2/s) is reached at about 3.7% of 3HV. This is indicated by the arrow in Fig. 9.

Saturation observed in Fig. 9 may be related to the random structure of the copolymers. Each chain bearing several 3HV units randomly distributed is thermally equivalent to each other in spite of the number of 3HV holding units. It seems that a pure kinetic magnitude such as thermal diffusivity is more sensitive to the micro environment than a thermodynamic or static magnitude such as thermal conductivity where the continuous 3HV mass addition rules a more linear trend. Additionally, DSC and density measurements would help to support the discussion of structural facts in the thermal behavior of the samples.

Acknowledgments

This work was partially supported by CNPq and FENORTE (RJ).

References

1. Rosencwaig, A. *Photoacoustics and Photoacoustic Spectroscopy* ; Wiley; New York, 1980.
2. Vargas, H.; Miranda, L.C.M. *Phys. Rep.* **1988**, *161*, 43.
3. Almond, D.; Patel, P. *Photoacoustics and Photothermal Science and Techniques*; Chapman and Hall; London, 1966.
4. Nery, J.W.; Pessoa Jr, O.; Vargas, H.; Reis, F.A.M.; Vinha, C.; Gabrielli, A.; Miranda, L.C. *Analyst* **1987**, *112*, 1487.
5. Anjo, A.M.; Moore, T.A. *Photobiology* **1984**, *39*, 635.
6. Busse, G. *Appl. Opt.* **1982**, *31*, 107.
7. Alvarado-Gil, J.J; Vargas, H.; Sanches-Sinencio, F.; Gonzales-Hernadez, J.; Miranda, L.C.M. *Opt. Eng.* **1997**, *36*, 348.
8. Calderon, A.; Alvarado-Gil, J.J; Gurevich, Y.G.; Cruz-Orea, A.; Delgadillo, I.; Vargas, H.; Miranda, L.C.M. *Phys. Rev. Lett.* **1997**, *25*, 5022.
9. Kinney, J.B.; Staley, R.H. *Annu. Rev. Mater. Sci.* **1992**, *12*, 295.
10. Doi, Y. *Microbial Polyesters*; VHC Publish; New York, 1990.
11. Lee, S.Y. *Tibtech.* **1996**, *14*, 431.
12. Anderson, A.J.; Dawes, E.A. *Microbiological Review* **1990**, *54*, 450.
13. Torres-Filho, A.; Leite, N.F.; Miranda, L.C.M.; Cella, N.; Vargas, H. *J. Appl. Phys.* **1989**, *66*, 97.
14. Cruz-Orea, A.; Delgadillo, I.; Vargas, H.; Guidino-Martins, A.; Vasques-Lopez C.; Calderon, A.; Alvarado-Gil, J.J. *J. Appl. Phys.* **1996**, *79*, 8951.
15. Ganguly P.; Sundrau, T.S. *Appl. Phys.* **1987**, *B43*, 43.
16. Touloukian, Y.S.; Powel, R.W.; Ho, C.Y.; Nicolassu, M.C. *Thermal Diffusivity*; IFI/Plenum, New York, 1973.
17. Charpentier, P.; Lepoutre, F.; Bertrand, L. *J. Appl. Phys.* **1982**, *53*, 608.
18. Leite, N.F.; Cella, N.; Vargas, H.; Miranda, L.C.M. *J. Appl. Phys.* **1987**, *61*, 3025.
19. Bluhm, L.; Hamer, G.K.; Marchessault, H.; Fyfe, C.A.; Varegin, R.P. *Macromolecules* **1986**, *19*, 287.
20. Mitomo, M.; Morishita, N.; Doi, Y. *Polymers* **1995**, *36*, 2573.
21. Eiermann, K.; Helleweg, K.H *J. Polymer Sci.* **1962**, *57*, 99.
22. Van Krevelen, D.W.; *Properties of Polymers*, 3rd Ed; Elsevier; Amsterdan, 1990.

Received: July 14, 1998